

1 **Operational POM increases are over-interpreted as SOM stabilization: Quantifying**  
2 **untransformed straw and biochar residues via magnetic separation**

3 Yuhan Xia<sup>a</sup>, Sen Dou<sup>a,\*</sup>, Song Guan<sup>a,\*</sup>, Dilimulati Yalihong<sup>a</sup>

4 <sup>a</sup>Key Laboratory of Soil Resource Sustainable Utilization for Commodity Grain Bases of Jilin  
5 Province, College of Resource and Environmental Science, Jilin Agricultural University,  
6 Changchun 130118, China

7 18543718988@163.com (Yuhan Xia); 17843098635@163.com (Dilimulati Yalihong).

8 \*Corresponding author.

9 Tel:13504486204, E-mail: dousen1959@126.com (Sen Dou); Tel:13504467990, E-mail:

10 guansong8888@163.com (Song Guan).

11 **Abstract**

12 Soil organic matter (SOM) is a complex mixture of organic compounds derived from the  
13 decomposition of plant and animal residues. SOM that has undergone microbial transformation  
14 and formed stable associations with minerals represents the stabilized fraction of soil organic  
15 carbon, which differs from the simple physical accumulation of external organic materials.  
16 Current understanding suggests that particulate organic matter (POM) includes both  
17 undecomposed and partially decomposed residues. Conventional analytical methods cannot  
18 clearly distinguish undecomposed exogenous organic residues from indigenous SOM.  
19 Consequently, increases in operationally defined POM are often misinterpreted as evidence of  
20 SOM stabilization or microbially transformed organic carbon formation. In this study, straw  
21 and biochar were magnetized through chemical coprecipitation and applied to the soil.  
22 Magnetic separation was performed at successive incubation times to isolate undegraded  
23 magnetic residues, thereby enabling more accurate tracking of SOM dynamics. Five treatments  
24 were established: blank control (CK), untreated straw (CS), untreated biochar with carbon input  
25 equivalent to straw (Bc), magnetized straw (MCS), and magnetized biochar (MBc). The  
26 recovery of magnetized straw residues declined continuously and reached 54.55% after 360 d,  
27 whereas biochar residues remained highly persistent at 92.48%. In the CS and Bc treatments,  
28 the organic carbon content of POM fractions and their proportion in total SOM were  
29 consistently higher than in CK, particularly during early incubation. However, after removing  
30 undegraded residues by magnetic separation, values were close to those of CK. This result  
31 indicates that the observed POM increases mainly originated from undecomposed external  
32 residues rather than microbially stabilized SOM. On day 30, the apparent increase in particulate

33 organic carbon (POC) was 63.48% in CS and 58.99% in Bc. Over time, the apparent POC  
34 increase in CS declined to 15.34% by day 360, whereas that in Bc remained high (53.71%).  
35 These findings suggest that interpreting total POM as stabilized or microbially transformed  
36 SOM may lead to misleading conclusions about SOM stability, particularly in short-term  
37 incubations or agroecosystems receiving fresh organic amendments. This study provides a  
38 basis for a more accurate evaluation of soil organic matter transformation dynamics and content.  
39 **Keywords:** Particulate Organic Matter (POM); Soil Organic Matter (SOM); Magnetic  
40 Materials; Straw; Biochar

## 41 **1. Introduction**

42 Soil organic matter (SOM) is a complex assemblage of organic compounds formed  
43 through the accumulation, decomposition and transformation of plant and animal residues. The  
44 decomposed part exhibits a much stronger binding capacity to soil minerals than  
45 undecomposed or partially decomposed residues. This strong binding makes it one of the most  
46 stable organic fractions in soil and supports its long-term persistence (Angst et al., 2021;  
47 Cotrufo et al., 2013; Dou et al., 2020; Vendig et al., 2023). Notably, the core of SOM refers to  
48 its labile and functional organic components with dynamic transformation properties. These  
49 components supply nutrients to the soil, sustain microbial activity, and regulate soil structure  
50 (Feng et al., 2025; Arumugam et al., 2025; Xu et al., 2026). Therefore, SOM should not be  
51 regarded merely as the passive accumulation of carbon-containing substances. Distinct SOM  
52 components exhibit different turnover rates and stabilization mechanisms (Sokol et al., 2022;  
53 Von Lützow et al., 2007). Cambardella and Elliott (1992) established a widely used particle-  
54 size fractionation method to separate SOM into particulate organic matter (POM, 2 mm to 53  
55  $\mu\text{m}$ ) and mineral-associated organic matter (MAOM,  $< 53 \mu\text{m}$ ). Based on these fractions,  
56 several conceptual models describing SOM formation and stabilization have been developed  
57 (Christensen, 1992; Cotrufo and Lavalley, 2022; Guo et al., 2022; Lavalley et al., 2020; Rocci  
58 et al., 2021; Witzgall et al., 2021).

59 In recent years, soil management and improvement measures have primarily aimed to  
60 increase organic material inputs and promote microbial utilization to form SOM (Cotrufo et al.,  
61 2013; Castellano et al., 2015). However, when application rates exceed microbial  
62 decomposition capacity, substantial amounts of undecomposed organic material can

63 accumulate in POM over a certain period (Bhattacharyya et al., 2011; Brown et al., 2014;  
64 Stewart et al., 2012), leading to sharp short-term increases in POM organic carbon content  
65 (Hua et al., 2022; Liang et al., 2016; Mitchell et al., 2018). This increase is transient and non-  
66 stabilized, as POM remains susceptible to decomposition and transformation even under the  
67 physical protection of soil (Connell et al., 2025), and such short-term increases exhibit low  
68 persistence in soil (Janzen, 2015; Powlson et al., 2014). Currently, an accurate assessment of  
69 the proportion and duration of this transient and non-stabilized, residue-derived increase in  
70 POM mass and organic carbon content at various times following organic material application  
71 is still lacking.

72 In routine experiments, methods such as heavy liquid separation, sieving, and electrostatic  
73 attraction can isolate some undecomposed organic materials. However, they are less effective  
74 for highly fragmented materials such as biochar, limiting evaluation of SOM transformation  
75 processes. Therefore, new approaches for efficient separation of undecomposed residues are  
76 required. Magnetized materials (e.g., iron-based materials such as nano-zero-valent iron and  
77 iron sulfides) can be rapidly separated from soil under an external magnetic field, enabling the  
78 efficient recovery of target substances (Li et al., 2024; Rana et al., 2025; Zhang et al., 2025).  
79 Although biochar modified with magnetized materials has been widely studied, most research  
80 has focused on heavy metal or pollutant adsorption, with no application in SOM transformation.  
81 Among magnetized material preparation methods, the chemical coprecipitation method has  
82 been widely used because of its operational simplicity, high efficiency, and ease of impurity  
83 removal (Zhou et al., 2019). It offers excellent biocompatibility, stability, and recyclability  
84 (Baragaño et al., 2020; Duan et al., 2022), which facilitate the combined application of organic

85 materials in soil. Iron particles form stable chemical bonds with organic materials, rather than  
86 simple physical adsorption. The surfaces of these materials contain abundant oxygen-  
87 containing functional groups such as hydroxyl, carboxyl, and carbonyl groups. During  
88 coprecipitation, these groups react with  $\text{Fe}^{2+}$  and  $\text{Fe}^{3+}$  to form coordinated and covalent bonds  
89 (Zhou et al., 2019; Duan et al., 2022). The resulting magnetic nanoparticles are uniformly  
90 embedded within the porous structure of the organic materials. This embedding prevents their  
91 detachment under non-biodegradation conditions, such as physical disturbance or soil  
92 hydration. When soil microorganisms decompose organic components, including cellulose,  
93 hemicellulose, and lignin, the functional groups that bind iron particles are disrupted. As a  
94 result, magnetic nanoparticles detach or disperse into non-magnetic fine particles smaller than  
95 10 nm, which cannot be captured by magnetic fields. Consequently, decomposed residues  
96 completely lose their magnetism (Li et al., 2024).

97 In this study, a chemical coprecipitation method was used to turn straw (CS) and straw  
98 biochar (Bc) into magnetized materials. At different incubation stages, undecomposed  
99 magnetized organic residues were separated using an external magnetic field to eliminate their  
100 interference in SOM determination. This approach allowed the accurate achievement of three  
101 objectives: (i) to quantify and characterize the incompletely decomposed residues at different  
102 times after organic material application; (ii) to determine the existence, proportion, and  
103 duration of residue-derived and non-stabilized accumulation in POM organic carbon; and (iii)  
104 to assess the proportion of organic residues ultimately transformed into stable SOM. The results  
105 provide critical support for precise evaluation of POM organic carbon content and elucidation  
106 of the mechanisms by which organic materials are transformed into stable SOM.

107

## 108 **2. Materials and Methods**

### 109 *2.1. Experimental materials*

110 The test soil was collected from the experimental station of Jilin Agricultural University,  
111 located in the semi-humid region of Northeast China (43°48'43.57"N, 125°23'38.50"E). The  
112 region has a temperate semi-humid climate, with an annual mean temperature of 4.6°C and  
113 average annual precipitation ranging from 600 to 700 mm. The soil is classified as Black Soil  
114 under the suborder of semi-moist temperature semi-eluvial soil in the Chinese soil  
115 classification system, which is equivalent to Argiudolls in the USDA soil taxonomy. In  
116 September 2023, 100 soil samples were randomly collected from the 0–20 cm layer using a  
117 soil auger and combined to form a composite sample. After sampling, visible organic residues  
118 were manually removed. The field-moist soil was air-dried and sieved through a 2 mm mesh  
119 for subsequent incubation. The basic properties of the soil were determined prior to the formal  
120 experiment as part of the initial soil characterization, with specific measurement methods  
121 following standard protocols in soil science: soil organic matter was determined by the  
122 dichromate oxidation method, total nitrogen by the Kjeldahl method, available nitrogen by the  
123 alkaline hydrolysis-diffusion method, available phosphorus by the molybdenum-antimony  
124 colorimetric method, and available potassium by flame photometry. The specific values were  
125 as follows: soil organic matter, 22.76 g kg<sup>-1</sup>; total nitrogen, 1.28 g kg<sup>-1</sup>; available nitrogen,  
126 132.21 mg kg<sup>-1</sup>; available phosphorus, 18.52 mg kg<sup>-1</sup>; and available potassium, 99.32 mg kg<sup>-1</sup>.

127 The corn stover (CS) used in the experiment was obtained from the Experimental Station  
128 of the Jilin Agricultural University, Jilin Province, China (Changchun, China). The entire CS

129 was rinsed with deionized water to remove surface ash and soil, dried in an oven for 24 h,  
130 ground using a grinder, and sieved through a 20-mesh sieve for later use.

131 The sieved straw powder (passing 20 mesh) was placed in a tubular furnace and pyrolyzed  
132 at 500°C for 2 h under a nitrogen atmosphere at a heating rate of 5°C min<sup>-1</sup>. After cooling to  
133 room temperature, the resulting black solid was collected as straw biochar (Bc) for further use.

134 The magnetized straw (MCS) and magnetized biochar (MBc) were prepared using the  
135 chemical coprecipitation method (Zhou et al., 2019) as follows: 2.5 g of FeCl<sub>3</sub>·6H<sub>2</sub>O and 1.5 g  
136 of FeSO<sub>4</sub>·7H<sub>2</sub>O (Fe<sup>3+</sup>:Fe<sup>2+</sup> molar ratio of 2:1) were weighed into a beaker. Subsequently, 2.0 g  
137 of dried CS or Bc was introduced to 100 mL of ultrapure water. The mixture was thoroughly  
138 stirred at room temperature for 30 s using a magnetic stirrer. An excess of ammonia solution  
139 (NH<sub>3</sub>·H<sub>2</sub>O) was subsequently added to adjust the pH to 10. After the reaction, the magnetic  
140 materials in the suspension were separated from the liquid phase using an external magnet. The  
141 magnetized samples were collected, dried in a vacuum oven at 60°C, weighed, and designated  
142 as magnetized straw (MCS) and magnetized biochar (MBc).

143

## 144 *2.2. Experimental Design*

145 Prior to the incubation experiment, the collected soil was pretreated by thorough mixing  
146 and sieving through a 2 mm mesh. Fine roots and other visible plant residues were carefully  
147 removed, and all iron-containing particles were extracted using a magnetic rod to minimize  
148 potential experimental interference. The study included five treatments: (1) control (CK): no  
149 organic amendment; (2) straw treatment (CS): non-magnetized straw; (3) biochar treatment  
150 (Bc): non-magnetized biochar with carbon content equivalent to CS; (4) magnetized straw

151 treatment (MCS): magnetized straw at the same carbon input as CS; and (5) magnetized biochar  
152 treatment (MBc): magnetized biochar with carbon equivalent to CS.

153 For each treatment, the respective materials (CS, Bc, MCS, and MBc) were thoroughly  
154 mixed with soil. Specifically, 400 g of soil was placed in PVC containers, and amendments  
155 were applied based on a full straw return rate of 11 t ha<sup>-1</sup>. Accordingly, 1.95 g of straw was  
156 added to the CS treatment, while 1.16 g of biochar was applied to the Bc treatment to match  
157 the carbon input of straw. The amount of magnetized straw and magnetized biochar were  
158 adjusted according to their preparation yields, resulting in 2.67 and 1.63 g for the MCS and  
159 MBc treatments, respectively.

160 To ensure homogeneous mixing, a small portion of amendment and air-dried soil was first  
161 combined in a glass beaker using a plastic spoon. After thorough mixing, the remaining soil  
162 was gradually added and continuously mixed until a uniform soil amendment mixture was  
163 obtained (Shi et al., 2024). The CK, CS, and Bc treatments each included three replicates. Each  
164 of the MCS and MBc treatments had six replicates divided into two subgroups: three without  
165 magnetic residue separation (MCS-O and MBc-O) and three with magnetic residue separation  
166 prior to soil and parameter analyses (MCS-D and MBc-D). During incubation, soil moisture  
167 was maintained at 25% by frequent weighing and watering, and all samples were incubated at  
168 30°C in a constant-temperature incubator.

169 The incubation began in April 2024, with destructive sampling at 30, 60, 180, and 360 d  
170 after the start. The samples from each treatment were retrieved, air-dried, and sieved through a  
171 2 mm mesh for subsequent analyses.

172

### 173 2.3. Fractionation of POM and MAOM

174 SOM was fractionated into particulate organic matter (POM) and mineral-associated  
175 organic matter (MAOM) following the wet sieving and particle-size fractionation methods  
176 described by Cambardella and Elliott (1992). Specifically, 20 g of air-dried soil was weighed  
177 and mixed with 60 mL of 5 g L<sup>-1</sup> sodium hexametaphosphate solution. The mixture was shaken  
178 for 18 h at 25°C and 180 rpm. The dispersed suspension was then passed through a 53 µm sieve  
179 and washed repeatedly with small volumes of deionized water until the filtrate became clear  
180 and colorless. The material retained on the sieve (>53 µm) was considered as sand particles  
181 and POM, while the fraction passing through the sieve (<53 µm) consisted of silt- and clay-  
182 sized particles along with MAOM.

183 The POM and MAOM fractions were collected separately in glass beakers. Within the  
184 soil-water suspension, a strong external magnetic iron rod was used to separate undecomposed  
185 magnetized straw and magnetized biochar residues from the POM and MAOM fractions in  
186 liquid form. These separated materials were designated as magnetized residue components  
187 within the POM and MAOM fractions, respectively. Both the soil fractions and magnetized  
188 residue fractions of POM and MAOM were dried at 60°C, weighed, and ground through a 60-  
189 mesh sieve (Liu et al., 2024). After the complete removal of undecomposed magnetized organic  
190 residues, preliminary determination of the organic carbon content in the original soil was  
191 performed using the potassium dichromate oxidation method with external heating (Nelson and  
192 Sommers, 1982). For formal and consistent characterization across all sample types, the soil  
193 organic carbon (SOC) content of the original soil, organic residue samples, and soil fractions  
194 collected at different incubation stages was subsequently measured with an elemental analyzer

195 (Vario EL III, Hanau, Germany). All organic carbon data reported in this study were obtained  
 196 from elemental analysis and corrected to an ash-free and moisture-free basis (Ndzelu et al.,  
 197 2021). To quantify the particulate organic carbon (POC) derived from amendment residues and  
 198 its contribution to total soil organic carbon (SOC), the following equations were applied:

$$199 \quad POC = M_p / 100 \times OC_p \quad (1)$$

$$200 \quad POM - C \text{ Contribution}(\%) = POC / SOC \times 100 \quad (2)$$

201 where  $M_p$  denotes the relative mass proportion of the POM fraction (%), i.e., percentage by  
 202 mass of POM in the soil sample),  $OC_p$  represents the organic carbon content of the POM  
 203 fraction ( $g\ kg^{-1}$ ), POC refers to the calculated particulate organic carbon content of the soil  
 204 sample ( $g\ kg^{-1}$ ), SOC denotes the total soil organic carbon content of the undisturbed soil ( $g$   
 205  $kg^{-1}$ ), and POM-C Contribution (%) represents the percentage contribution of particulate  
 206 organic carbon to total soil organic carbon.

207

#### 208 2.4. Calculation of organic residue retention rate

209 The cumulative retention rate of dry matter from straw (CS) and biochar (Bc) residues  
 210 within the MCS and MBc fractions was calculated as follows:

$$211 \quad L(\%) = \frac{M_d - M_{Fe}}{M_1} \times 100\% \quad (3)$$

212 where  $L$  is the mass retention rate of the organic residue (%),  $M_d$  is the dry mass of the recovered  
 213 magnetized material at different decomposition times (g),  $M_{Fe}$  is the dry mass of the Fe-related  
 214 products in the applied magnetized material (g), and  $M_1$  is the dry mass of the unmagnetized  
 215 straw or biochar applied in the CS and Bc treatments (g). For the magnetized treatments (MCS  
 216 and MBc), the applied mass of magnetized materials was calculated based on the same  $M_1$  to

217 ensure equal organic carbon input across all treatments.

218

## 219 *2.5. Data analysis*

220 All data were first organized using Microsoft Office Excel 2022, followed by statistical  
221 analysis with IBM SPSS Statistics 25 (IBM Corporation, Armonk, NY, USA). One-way  
222 analysis of variance (ANOVA) was performed to examine differences in the measured indices  
223 across all treatments and incubation time points, with post-hoc multiple comparisons conducted  
224 using the least significant difference (LSD) test at the 0.05 significance level. Additionally,  
225 two-way ANOVA was applied to evaluate the effects of treatment, incubation time, and their  
226 interaction on soil and fraction-specific organic carbon contents, and Duncan's multiple range  
227 test (integrated in SPSS) was used for post-hoc comparison of significant differences. Graphs  
228 were generated using Origin 2022.

229

## 230 **3. Results and analysis**

### 231 *3.1. Differences between magnetized and original organic materials*

232 As shown in Table 1, no significant differences were observed in the molar ratios of  
233 carbon to nitrogen (C/N), hydrogen to carbon (H/C), or oxygen to carbon (O/C) before and  
234 after magnetic modification of the organic materials. This result indicates that the  
235 magnetization process does not substantially alter the elemental composition of organic  
236 materials. The C/N, H/C, and O/C ratios serve as key indicators of the chemical properties and  
237 structural characteristics of organic materials. Specifically, the C/N ratio could be closely  
238 associated with the decomposition rate of organic substrates, the H/C ratio reflects aromaticity,

239 and the O/C ratio represents the oxidation level (Ndzelu et al., 2021). The near-constant values  
 240 of these ratios before and after magnetization suggest that the fundamental chemical attributes  
 241 and structural features of the organic materials remained unchanged by magnetic treatment.

242 The metallic nanoparticles produced by coprecipitation were uniformly distributed on the  
 243 surfaces of straw and biochar within a narrow size range. They formed a discontinuous and  
 244 porous coating, rather than a dense and impermeable layer. This nanoscale coating does not  
 245 block surface functional groups or internal pore structures, thereby preserving the natural  
 246 accessibility of organic materials to soil microorganisms (Panda et al., 2026). As a result, the  
 247 decomposition behavior of the magnetized materials remained consistent with that of the  
 248 unmodified materials, supporting their reliability in tracking SOM transformation processes.  
 249 Therefore, the magnetized organic materials exhibited high chemical and structural consistency  
 250 with their non-magnetized counterparts, making them reliable representatives of original  
 251 organic substrates. This conclusion could present a sound theoretical basis for using  
 252 magnetized organic materials in subsequent experiments to investigate the behavior of  
 253 undecomposed organic residues in soil. It also ensured the reliability and accuracy of results  
 254 related to the assessment of residue-driven increases in soil organic matter through the  
 255 separation of magnetized organic residues.

256

257 **Table 1** Comparison of elemental composition of organic materials before and after  
 258 magnetization.

Treatment	N	C	H	O	C/N	H/C	O/C
	%				Ratio	Ratio	Ratio

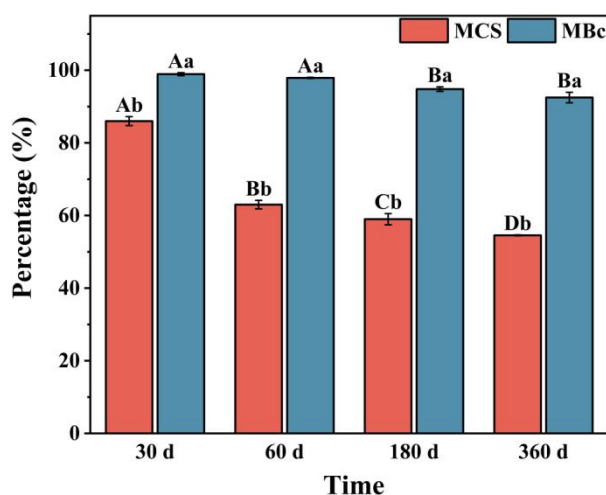
CS	0.99	46.20	6.84	45.96	54.32	1.78	0.75
Bc	0.78	79.35	3.65	16.22	118.49	0.55	0.15
MCS	1.00	46.68	6.55	45.77	54.43	1.68	0.74
MBc	0.80	79.37	3.54	16.30	115.65	0.53	0.15

259

### 260 3.2. Temporal changes in magnetized organic residues in soil

261 As shown in Fig. 1, the retention rate of straw residues in MCS gradually decreased over  
 262 the incubation period, with values of 85.98%, 63.00%, 58.99%, and 54.55% at 30, 60, 180, and  
 263 360 d, respectively. In contrast, the biochar fraction in MBc exhibited relatively minor changes,  
 264 with retention rates of 98.92%, 97.88%, 94.80%, and 92.48% at the corresponding time points.  
 265 These results show that the straw fraction in MCS decomposed gradually in soil over the  
 266 incubation duration, and was gradually transformed into relatively recalcitrant organic matter.  
 267 Conversely, the biochar fraction in MBc was significantly more resistant to microbial  
 268 decomposition and more persistent than straw throughout the experiment, as evidenced by its  
 269 consistently higher residue rate (92.48% at 360 d) compared to straw (54.55% at 360 d).

270



271

272 **Fig. 1.** Residual rates of undecomposed magnetized straw (MCS) and magnetized biochar

273 (MBc) separated from soil at different incubation times.

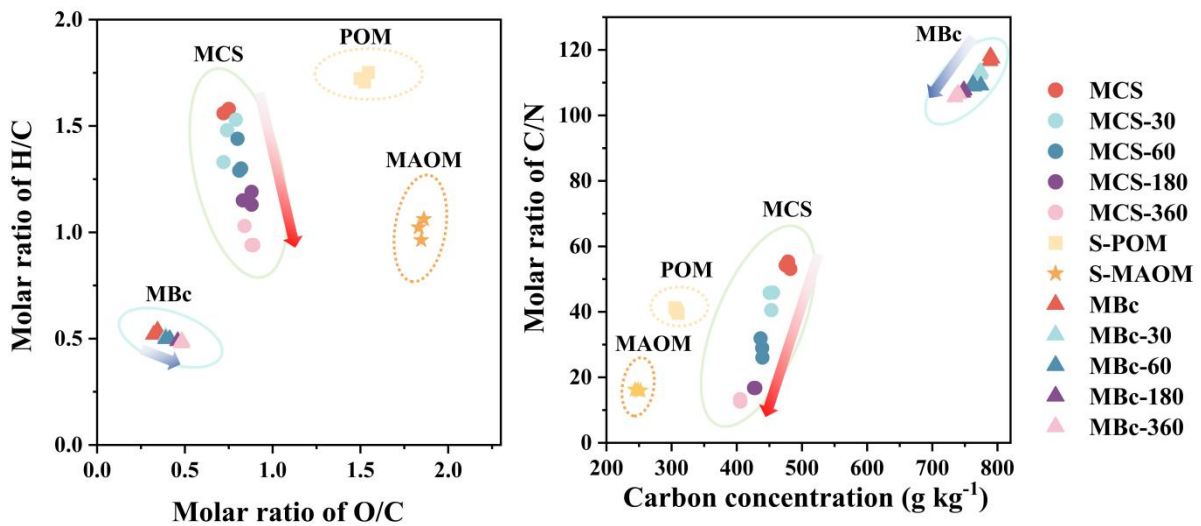
274 Note: MCS refers to magnetized straw; MBc refers to magnetized biochar. Different uppercase  
275 letters indicate significant differences among sampling times within the same organic residue  
276 ( $p < 0.05$ ), while different lowercase letters indicate significant differences between organic  
277 residues at the same sampling time ( $p < 0.05$ ).

278

279 The results in Fig. 2 further demonstrate that the two types of magnetized organic  
280 materials differed not only in their retention rates but also in the extent of mass changes after  
281 decomposition. Compared with the soil MAOM fraction, undecomposed MCS residues in the  
282 early incubation stage exhibited higher H/C and C/N ratios, closer to those of the soil POM  
283 fraction. As shown in Fig. 2a, the H/C ratio of MCS residues decreased gradually over time,  
284 approaching that of MAOM by day 360, whereas the O/C ratio exhibited a slow increase. In  
285 contrast, these trends were not evident in MBc residue samples. A decrease in the H/C ratio  
286 indicates a reduced aliphatic character of the organic residues (Banach-Szott et al., 2014; Dou  
287 and Li, 2010), while an increase in the O/C ratio could reflect increased oxidation (Mohammed  
288 et al., 2023). These findings indicate that with prolonged incubation, shifts in the H/C and O/C  
289 ratios of the organic residues (evident from the bulk elemental analysis presented in Fig. 2) are  
290 consistent with oxidative transformation and changes in aliphatic content and structural  
291 condensation of the organic material. Fig. 2b further shows that the C/N ratio and carbon  
292 concentration of MCS residues declined continuously, gradually approaching those of the soil  
293 MAOM fraction. This trend reflects the progressive decomposition and transformation of  
294 organic residues toward chemical characteristics similar to those of native soil mineral-

295 associated organic matter, consistent with observations of organic matter stabilization in  
 296 previous studies (Abakumov and Eskov, 2023). Notably, the C/N ratio of MCS residues at 360  
 297 d approximated that of MAOM. Conversely, the changes in these parameters for MBc residues  
 298 were relatively small, indicating that the organic components of MBc residues were more  
 299 resistant to microbial decomposition and transformation than straw residues within the 360-  
 300 day incubation period.

301



302

303 **Fig. 2.** Van Krevelen diagram of atomic H/C and O/C ratios (a), and comparison of C/N ratio  
 304 and carbon concentration (b) of magnetized organic residues, soil POM, and MAOM fractions  
 305 at different incubation times.

306 Note: MCS refers to magnetized straw; MBc refers to magnetized biochar. MCS-30, MCS-60,  
 307 MCS-180, and MCS-360 represent undecomposed magnetized straw residues separated from  
 308 soil at 30, 60, 180, and 360 days, respectively; MBc-30, MBc-60, MBc-180, and MBc-360  
 309 represent undecomposed magnetized biochar residues separated from soil at the same  
 310 respective time points. S-POM and S-MAOM denote soil samples of particulate organic matter  
 311 and mineral-associated organic matter fractions, respectively. All data are corrected on an ash-

312 free and moisture-free basis.

313

314 *3.3. Organic residues cause residue-derived increases in the mass proportion and organic*  
315 *carbon content of soil POM fraction*

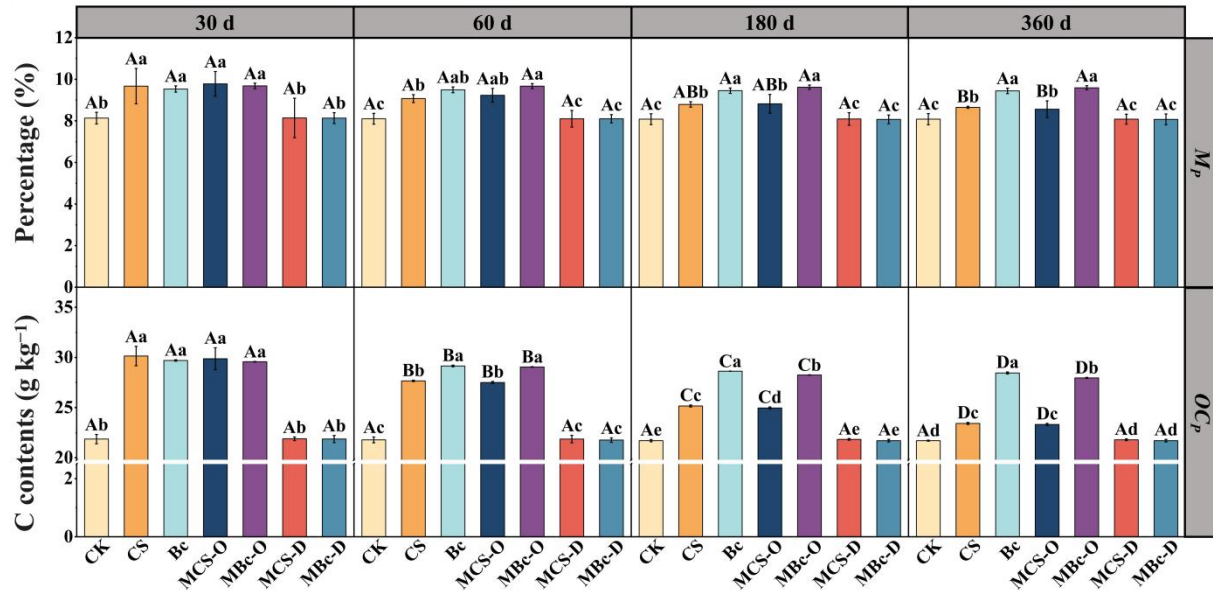
316 Fig. 3 presents the relative mass proportions of the soil POM fraction at different  
317 incubation times across treatments. Clear differences among treatments were evident. Two-  
318 way ANOVA (Table S1) revealed that the relative mass proportion of the POM fraction ( $M_P$ )  
319 was significantly affected by treatment ( $p < 0.001$ ) and incubation time ( $p < 0.01$ ), with no  
320 significant interaction between treatment and time ( $p > 0.05$ ). Similarly, as shown in Fig.3, the  
321 organic carbon content of the POM fraction ( $OC_P$ ) was significantly influenced by treatment  
322 ( $p < 0.001$ ), incubation time ( $p < 0.001$ ), and their interaction ( $p < 0.001$ ). Notably, no significant  
323 differences were observed between the MCS-O and MBc-O (magnetized treatments without  
324 removing magnetic organic residues at harvest) and the CS and Bc treatments at any sampling  
325 time, supporting the applicability of magnetized materials in soil applications.

326 At 30, 60, 180, and 360 d of incubation, the mass proportion of the POM fraction ( $M_P$ ) in  
327 the CS treatment increased by 18.94%, 11.97%, 8.78%, and 7.05%, respectively, compared  
328 with CK. For the Bc treatment, the corresponding increases were 17.22%, 17.16%, 16.95%,  
329 and 16.83%, respectively. However, after the removal of magnetized organic residues from the  
330 soil, no significant changes in POM mass proportion were observed in the MCS-D and MBc-D  
331 (magnetized treatments with magnetic organic residues removed before analysis) treatments  
332 compared with CK. These results indicate that the increases in POM mass proportion observed  
333 in the CS and Bc treatments were residue-driven increases, arising from the retention of

334 persistent amendment residues within the operationally defined  $>53 \mu\text{m}$  particulate fraction.  
335 Further analysis revealed that in the CS treatment, this residue-driven elevation decreased  
336 gradually over time, stabilizing at approximately day 180, whereas in the Bc treatment, it  
337 remained nearly constant throughout the incubation period.

338 Similarly, at different time points, the organic carbon content of the POM fraction ( $OC_P$ )  
339 in the CS treatment increased by 37.87%, 26.99%, 15.94%, and 7.92%, respectively, compared  
340 with CK. For the Bc treatment, the increases were 35.86%, 33.83%, 31.93%, and 31.10%,  
341 respectively. At the same time points, the  $OC_P$  in the CS treatment exceeded that in the MCS-  
342 D treatment by 37.68%, 26.53%, 15.25%, and 7.48%, respectively. Moreover, the  $OC_P$  in the  
343 Bc treatment was higher than in the MBc-D treatment by 35.80%, 33.96%, 31.93%, and  
344 31.10%. These results demonstrated that both the carbon content and mass proportion of the  
345 POM fraction exhibited residue-driven increases, resulting from the retention of persistent  
346 amendment residues within the operationally defined  $>53 \mu\text{m}$  particulate fraction. As no  
347 significant difference was identified between the MCS-D and CK treatments, the reduction in  
348 the residue-derived increase for the CS treatment was attributable not to an increase in organic  
349 carbon content in the MCS-D treatment but to the decomposition of organic residues within  
350 the fraction.

351



352

353 **Fig. 3.** Relative mass proportion ( $M_p$ ) and organic carbon content ( $OC_p$ ) of the soil POM  
 354 fraction at different incubation times across treatments.

355 Note: CK denotes the control treatment without organic amendments; CS denotes the treatment

356 with normal straw application; Bc denotes the treatment with biochar applied at an equivalent

357 carbon amount to straw; MCS denotes the treatment with magnetized straw applied at an

358 equivalent carbon amount; and MBc denotes the treatment with magnetized biochar applied at

359 an equivalent carbon amount. MCS-O and MBc-O refer to treatments in which magnetized

360 organic materials were not removed at the end of incubation; MCS-D and MBc-D refer to

361 treatments in which magnetized organic residues were separated from the soil before testing

362 the remaining soil samples. Different uppercase letters indicate significant differences among

363 sampling times within the same treatment, whereas different lowercase letters indicate

364 significant differences among treatments at the same sampling time ( $p < 0.05$ ).

365

### 366 3.4. Organic residues cause residue-derived increases in POC and SOC contents

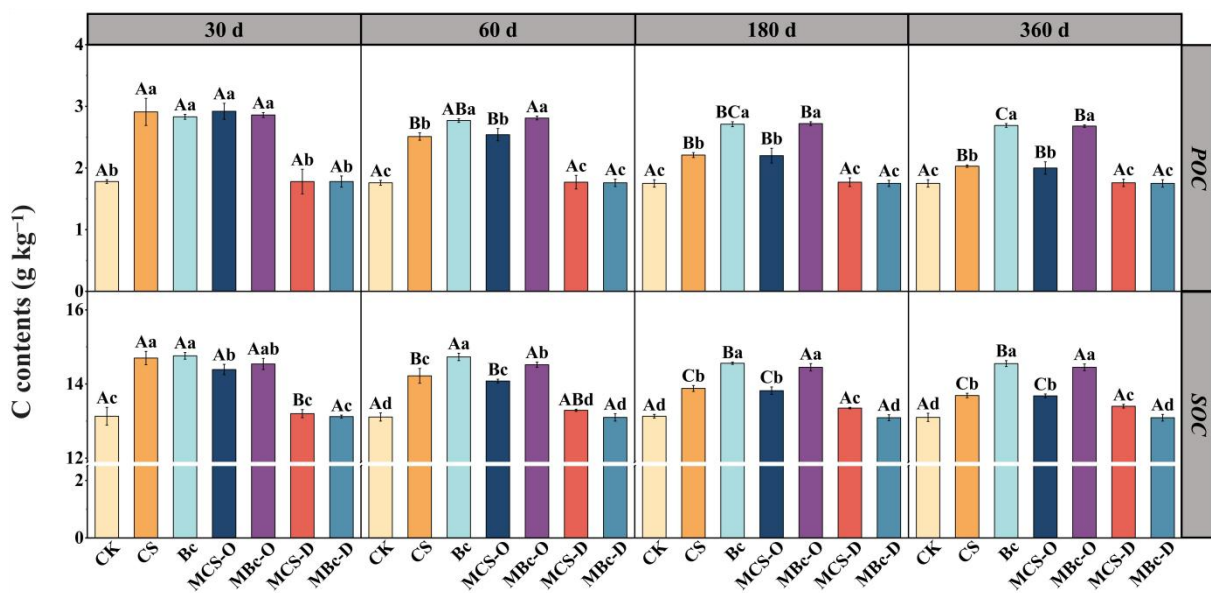
367 As shown in Fig. 4 and Table S2, two-way ANOVA indicated that the POC content was

368 significantly affected by treatment ( $p < 0.001$ ), incubation time ( $p < 0.001$ ), and their interaction  
369 ( $P < 0.001$ ). Similarly, the SOC content was significantly influenced by treatment ( $p < 0.001$ ),  
370 incubation time ( $p < 0.001$ ), and their interaction ( $p < 0.001$ ). The POC contents in the MCS-O  
371 and MBc-O treatments were slightly lower than those in the CS and Bc treatments, although  
372 the differences were not statistically significant. Specifically, at 30, 60, 180, and 360 d of  
373 incubation, the POC contents in both the CS and Bc treatments were significantly higher than  
374 those in CK. The increase in POC content compared with CK in the CS treatment showed a  
375 clear decreasing trend, with increases of 63.48%, 42.61%, 26.29%, and 16.00%, respectively.  
376 In contrast, although the POC content in the Bc treatment also declined during incubation, the  
377 decrease was less pronounced, with increases of 58.99%, 57.38%, 54.86%, and 53.71% at the  
378 respective time points. No significant differences in POC content were observed between the  
379 MCS-D and MBc-D treatments, indicating that the elevated POC contents in the CS and Bc  
380 treatments originated from undecomposed organic residues. The POC contents in the CS  
381 treatment exceeded that in the MCS-D treatment by 63.48%, 41.80%, 24.86%, and 15.34% at  
382 the respective time points, whereas the POC contents in the Bc treatment were higher than that  
383 in the MBc-D treatment by 58.99%, 42.61%, 54.86%, and 53.71%, respectively.

384 Across all incubation periods, the SOC contents in the MCS-O and MBc-O treatments  
385 were comparable to those in the CS and Bc treatments, indicating strong consistency between  
386 the magnetized organic materials and the original organic materials during incubation.  
387 Specifically, at 30, 60, 180, and 360 d, the SOC contents in the CS and Bc treatments were  
388 significantly higher than in CK. The SOC content in the CS treatment showed a decreasing  
389 trend, with increases of 11.95%, 8.40%, 5.71%, and 4.50%, respectively. In contrast, although

390 the *SOC* content in the Bc treatment also declined over time, the decrease was less pronounced,  
 391 with increases of 12.41%, 12.35%, 10.89%, and 11.06% at the respective time points. After  
 392 360 d of incubation, the *SOC* content in the MCS-D treatment showed an increasing trend,  
 393 whereas the *SOC* content in the MBc-D treatment remained similar to that in CK without  
 394 significant changes, maintaining a relatively stable level throughout the incubation period.

395



396

397 **Fig. 4.** *POC* and *SOC* contents of different treatments at various incubation times.

398 Note: CK denotes the control treatment without organic amendments; CS denotes the treatment  
 399 with normal straw application; Bc denotes the treatment with biochar applied at an equivalent  
 400 carbon amount to straw; MCS denotes the treatment with magnetized straw applied at an  
 401 equivalent carbon amount; and MBc denotes the treatment with magnetized biochar applied at  
 402 an equivalent carbon amount. MCS-O and MBc-O refer to treatments in which magnetized  
 403 organic materials were not removed at the end of incubation; MCS-D and MBc-D refer to  
 404 treatments in which magnetized organic residues were separated from the soil before testing  
 405 the remaining soil samples. Different uppercase letters indicate significant differences among

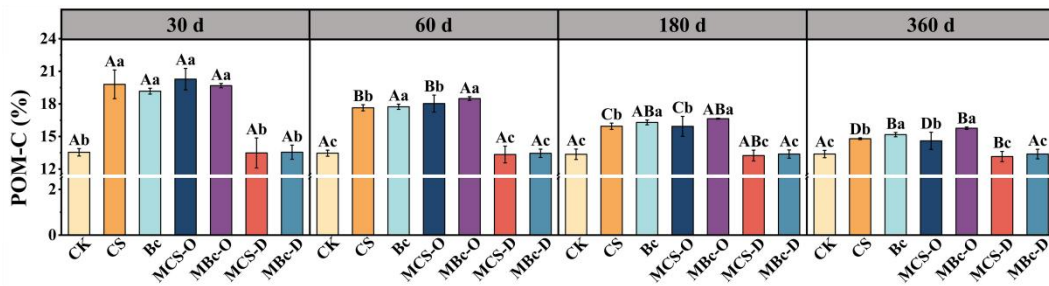
406 sampling times within the same treatment, whereas different lowercase letters indicate  
407 significant differences among treatments at the same sampling time ( $p<0.05$ ).

408

### 409 *3.5. Organic residues cause residue-derived increases in the proportion of POM in total SOM*

410 As shown in Fig. 5 and Table S3, two-way ANOVA revealed that the contribution of POC  
411 to total SOC (POM-C contribution, POC/SOC) was significantly affected by treatment  
412 ( $p<0.001$ ), incubation time ( $p<0.001$ ), and their interaction ( $p<0.001$ ). POM-C in the CS and  
413 Bc treatments was significantly higher than that in CK. At different incubation times, the ratios  
414 in the CS treatment increased by 46.23%, 31.05%, 19.31%, and 10.54%, whereas those in the  
415 Bc treatment increased by 41.58%, 39.60%, 39.15%, and 38.04%, respectively. However, the  
416 residue-driven elevation of the POM proportion in SOM persisted. At different time points, the  
417 ratios in the CS treatment were 46.88%, 32.23%, 20.39%, and 12.47% higher than those in the  
418 MCS-D treatment, whereas in the Bc treatment, they were 41.47%, 39.70%, 38.94%, and  
419 38.04% higher than those in the MBc-D treatment. Notably, the POM proportion in SOM in  
420 the MCS-D treatment was lower than that in CK, which was attributed to the greater conversion  
421 of straw residues into MAOM during decomposition, thereby increasing the MAOM  
422 proportion in SOM. In contrast, no significant changes were observed in biochar in the MBc-  
423 D treatment, and the proportion of POM in SOM was similar to that in CK.

424



425

426 **Fig. 5.** Proportion of POM-C contribution (POC/SOC) for different treatments at various

427 incubation times.

428 Note: CK denotes the control treatment without organic amendments; CS denotes the treatment

429 with normal straw application; Bc denotes the treatment with biochar applied at an equivalent

430 carbon amount to straw; MCS denotes the treatment with magnetized straw applied at an

431 equivalent carbon amount; and MBc denotes the treatment with magnetized biochar applied at

432 an equivalent carbon amount. MCS-O and MBc-O refer to treatments in which magnetized

433 organic materials were not removed at the end of incubation; MCS-D and MBc-D refer to

434 treatments in which magnetized organic residues were separated from the soil before testing

435 the remaining soil samples. Different uppercase letters indicate significant differences among

436 sampling times within the same treatment, whereas different lowercase letters indicate

437 significant differences among treatments at the same sampling time ( $p < 0.05$ ).

438

#### 439 **4. Discussion**

##### 440 *4.1. Differences in the transformation of organic materials with different qualities in soil*

441 As shown in Fig. 1, the proportion of undecomposed straw residues significantly

442 decreased over different incubation periods, with a residue rate of only 54.55% after 360 d. In

443 sharp contrast, biochar exhibited almost no decomposition, maintaining a high residue rate of

444 92.48%. Based on the bulk elemental analysis in Fig. 2, the organic straw component within

445 magnetic straw residues underwent progressive oxidative transformation and structural  
446 condensation with incubation time, as reflected by the gradual shifts in H/C and O/C ratios,  
447 indicating a gradual evolution toward more chemically stable characteristics. Meanwhile, the  
448 magnetic mineral phase remained preserved, resulting in the persistent magnetic properties of  
449 the residual materials. By contrast, MBc residues exhibited negligible changes in elemental  
450 composition throughout the incubation period.

451       The contrasting decomposition dynamics between straw and biochar are primarily driven  
452 by their inherent structural differences. Straw contains abundant labile components (e.g.,  
453 carbohydrates, organic acids, and amino acids) that are readily utilized by soil microorganisms,  
454 leading to rapid mineralization within 0–60 d, followed by slower decomposition of recalcitrant  
455 aromatic and polymeric fractions during 60–180 d, which aligns with the present findings and  
456 previous reports (Chen et al., 2010; Ren et al., 2021). In contrast, biochar is produced via  
457 pyrolysis of biomass at 300–700°C under anaerobic conditions (Dungait et al., 2012); during  
458 this process, labile cellulose-C in straw is converted into aromatic biochar-C with highly  
459 condensed structures, greatly enhancing its structural stability and resistance to microbial  
460 decomposition in soil (Yin et al., 2022), thus enabling biochar to remain largely as a residue  
461 (Bornø et al., 2019). Although straw has a lower C/N ratio than biochar, this difference is a  
462 secondary feature accompanying their distinct chemical structures, rather than the dominant  
463 factor controlling their decomposition rates.

464       The high stability of biochar observed in this study confirms its unique advantages as a  
465 carbon-rich soil amendment for soil carbon sequestration and structural improvement, which  
466 is consistent with previous studies (Cao et al., 2022; Fan et al., 2021; Wang et al., 2025; Zhang

467 et al., 2024). Characterized by slow decomposition and a surface conducive to organic  
468 molecule aggregation, biochar can effectively reduce soil bulk density (Zhang et al., 2021),  
469 increase soil porosity (He et al., 2022), alleviate soil acidification (Shi et al., 2023), retain soil  
470 moisture (Khaledi et al., 2023), and enhance nutrient absorption efficiency and nutrient cycling  
471 coordination (Burgeon et al., 2022) when applied to soil. Therefore, despite its slow  
472 decomposition in soil, biochar plays a significant role in improving soil structure and function,  
473 which is further supported by its high persistence observed in the present one-year incubation  
474 experiment.

#### 475 *4.2. Residual undecomposed organic matter contributes to increases in the POM fraction*

476 The analysis of the weight proportion and organic carbon content of soil fractions  
477 presented in Figs. 3 and 4 clearly demonstrated that under the CS and Bc treatments, both the  
478 relative mass and organic carbon content of the POM fraction were consistently higher than  
479 those in the CK treatment. This finding aligns with those reported by Xie et al. (2014). The  
480 POM fraction, a valid component of soil organic matter (SOM), mainly consists of partially  
481 decomposed, chemically recalcitrant polymeric structures, such as acid-insoluble fibers formed  
482 through fragmentation, which could primarily originate from exogenous organic materials.  
483 Owing to its rapid responsiveness to environmental changes, POM can be highly sensitive to  
484 agricultural management practices (Christensen, 1992; Cotrufo et al., 2022; Guo et al., 2022;  
485 Rocci et al., 2021; Witzgall et al., 2021). Xie et al. demonstrated that increasing the input of  
486 organic materials directly influenced both SOM content and its proportion within the POM  
487 fraction. They attributed this phenomenon to the continuous accumulation of organic residues  
488 in soil induced by organic amendments (Xie et al., 2014). However, it is critical to distinguish

489 between POM derived directly from undecomposed amendment residues and MAOM formed  
490 through microbial transformation of organic materials. This distinction clarifies the dynamic  
491 nature of SOM accumulation. It does not imply that residue-derived POM is an invalid  
492 component of SOM.

493 In this experiment, the POM mass proportion and organic carbon content for the MCS-D  
494 and MBc-D treatments were obtained by first applying the magnetic materials to the soil for a  
495 period of incubation, then extracting the magnetic residues from the soil, and subsequently  
496 testing the soil samples after removal of the undecomposed materials. The results showed that  
497 after the magnetic materials were extracted, the POM mass proportion and organic carbon  
498 content in the MCS and MBc treatments did not exhibit significant increases compared with  
499 the CK treatment. This proved that the increases in POM mass proportion and organic carbon  
500 content observed under the CS and Bc treatments were largely attributable to the direct input  
501 of straw and biochar materials, with most undecomposed organic residues remaining within  
502 the POM fraction. Moreover, the residue-driven increases in both POM mass proportion and  
503 organic carbon content under the CS treatment decreased over the incubation period, whereas  
504 the corresponding values under the Bc treatment remained nearly constant. These findings  
505 suggest that the quantity, quality, and incubation duration of organic residues are key factors  
506 driving the increase in the POM mass proportion and organic carbon content. Additionally, the  
507 extent of increase in the POM fraction was closely related to the amount and source of organic  
508 material applied.

509 The results shown in Fig. 4 revealed a pronounced decreasing trend in the POM fraction  
510 organic carbon content (POC) under CS treatment. This confirmed that the effect of organic

511 material addition in the short term was predominantly reflected in the POM fraction, whereas  
512 a gradual increase in the MAOM fraction was observed. This aligned with the conclusions of  
513 Bhattacharyya et al. (2011), Brown et al. (2014), and Stewart et al. (2012) who reported that  
514 organic amendments were primarily retained in the POM fraction, which could be more prone  
515 to mineralization, while gains in the MAOM fraction remained limited. The MAOM fraction  
516 in soil is widely regarded as being predominantly formed over decadal to centennial timescales  
517 through long-term weathering processes involving interactions between organic matter and  
518 secondary minerals. Notably, MAOM can also be produced via biotic processes (e.g.,  
519 earthworm activities) over much shorter timescales. Due to this extremely slow formation  
520 process, MAOM accumulation can be difficult to achieve in the short term (Kleber et al., 2007;  
521 Slessarev et al., 2022). Moreover, because microorganisms struggle to utilize chemically  
522 recalcitrant components within plant residues, decomposition of these highly processed  
523 structural organic residues and POM components has been reported to cause MAOM formation  
524 (Cotrufo et al., 2015). This explains why the organic carbon data for the Bc treatment in this  
525 study (Figs. 3 and 4) indicated that most undecomposed organic residues remained preserved  
526 within the POM fraction. This also accounted for the consistently higher POM-C contribution  
527 observed in the CS and Bc treatments than in the MCS-D and MBc-D treatments.

528       Currently, some studies have suggested that abundant POM can be crucial for  
529 agroecosystem functioning and crop productivity, thereby advocating for greater research  
530 focusing on POM increments (Wood et al., 2016). However, the results of this study indicated  
531 that within the POM fraction, the dominant influencing factors were the quantity and quality  
532 of undecomposed organic residues, with temporal factors exerting a significant impact.

533 Although the POM fraction plays an important role in nutrient supply, microbial activity  
534 promotion, and soil structure regulation, the indiscriminate addition of organic materials to soil  
535 primarily increases the amount of undecomposed organic residues, most of which reside in the  
536 POM fraction over short time periods. This practice directly increases the measured SOM  
537 content. Notably, the observed short-term increase in soil organic carbon was primarily derived  
538 from undecomposed exogenous organic residues retained in the particulate organic matter  
539 (POM) fraction, rather than the formation of microbially processed and mineral-associated  
540 stable organic matter pools. These findings highlight the need to distinguish between residue-  
541 derived POM and microbially transformed MAOM when interpreting SOM measurements,  
542 particularly in short-term incubation studies. Without this distinction, assessments of SOM  
543 dynamics may overestimate the short-term residue-driven increases in POM. This could lead  
544 to misinterpretation of SOM stabilization and biased evaluation of stable soil carbon pools in  
545 systems receiving recent organic amendments.

546

## 547 **5. Conclusion**

548 Based on the comprehensive results of this study, magnetic treatment exerted minimal  
549 influence on the elemental composition of organic materials, indicating that magnetized  
550 organic materials can serve as valid representatives of normal organic materials and that the  
551 related experimental outcomes are reliable. The straw component in MCS decomposed readily  
552 in soil, with its residue rate markedly decreasing during the incubation period. The H/C ratio  
553 of the residues decreased, the O/C ratio increased, and both the C/N ratio and carbon  
554 concentration decreased continuously, indicating reduced aliphaticity, enhanced oxidation, and

555 a molecular structural shift toward increased aromaticity and enhanced structural stability.  
556 Furthermore, the proportion of residues in the POM fraction sharply declined with incubation  
557 time, approaching the characteristics of MAOM after 360 d. In contrast, the biochar component  
558 in MBc exhibited high stability in soil, showing minor changes in the residue rate, elemental  
559 ratios, and a relatively gradual decline in the proportion of the POM fraction, reflecting greater  
560 resistance to decomposition. After organic material addition, the accumulation of the  
561 operationally defined POM fraction is frequently regarded as an indicator of enhanced soil  
562 organic carbon sequestration or microbially mediated organic matter transformation. However,  
563 as a labile organic pool, the elevated POM observed in this study was largely derived from  
564 recalcitrant and untransformed exogenous amendment residues, rather than the formation of  
565 chemically stable soil organic matter. In this study, the presence of unseparated residues in the  
566 CS and Bc treatments resulted in higher POM organic carbon content and a greater proportion  
567 of total SOM than in CK. This effect was most pronounced during the early incubation period.  
568 After residue separation, the MCS-D and MBc-D treatments displayed little difference from  
569 CK, confirming that the observed POM increases were attributable to incompletely  
570 decomposed residues. On day 30, the residue-driven increases in POC content reached 63.48%  
571 and 58.99% for the CS and Bc treatments, respectively. Over time, the residue-driven increase  
572 in CS gradually diminished, decreasing to 15.34% after 360 d, whereas the residue-driven  
573 increase in Bc remained largely unchanged and stable, still reaching 53.71% after 360 d. Owing  
574 to the greater conversion of straw residues into MAOM during decomposition, the POM  
575 fraction contribution in MCS-D was lower than that in CK. Concurrently, biochar in MBc-D  
576 exhibited no significant change, with a POM contribution comparable to that of CK. These

577 results confirm the risk of overestimating stabilized soil organic carbon pools when residue-  
578 derived POM is included in the total SOM assessments. This risk is particularly evident in  
579 short-term incubation studies or agroecosystems receiving recent organic amendments,  
580 especially when incorporating pyrogenic carbon such as biochar. As a notable exception to the  
581 general lability of POM, such persistent recalcitrant materials can lead to an overestimation of  
582 soil organic matter stability, as their persistence arises from inherent chemical recalcitrance  
583 rather than microbially mediated stabilization processes. These findings provide a useful  
584 reference for the accurate evaluation of soil organic matter transformation processes and their  
585 content.

586

587 **Data availability:** The datasets and code used in this study are available from the  
588 corresponding author upon reasonable request.

589

590 **Conflicts of interest:** The authors declare no conflict of interest.

591

592 **CRedit authorship contribution statement:** Yuhan Xia: Writing – original draft,  
593 Visualization, Validation, Methodology, Investigation, Formal analysis, Data curation,  
594 Conceptualization. Sen Dou: Writing – review & editing, Supervision, Resources, Project  
595 administration, Methodology, Funding acquisition, Conceptualization. Guan Song: Writing –  
596 review & editing, Supervision, Resources, Project administration, Methodology, Funding  
597 acquisition, Conceptualization. Dilimulati Yalikhong: Writing – review & editing, Methodology,  
598 Investigation.

599

600 **Funding:** This work was supported by the National Key Research and Development Program  
601 of China (2024YFD1500502-04).

602

### 603 **References**

604 Abakumov, E., Eskov, A., 2023. Organic matter structural composition of vascular epiphytic  
605 suspended soils of South Vietnam. *Applied Sciences* 13, 4473.  
606 <https://doi.org/10.3390/app13074473>.

607 Angst, G., Mueller, K.E., Nierop, K.G.J., Simpson, M.J., 2021. Plant- or microbial-derived? A  
608 review on the molecular composition of stabilized soil organic matter. *Soil Biology and  
609 Biochemistry* 156, 108189. <https://doi.org/10.1016/j.soilbio.2021.108189>.

610 Arumugam, T., Kinattinkara, S., Vellingiri, K., Arumugam, M., Rajamani, J., Jayaseelan, A.,  
611 2025. Assessment of agricultural soil quality in macro and micronutrient analysis of  
612 Kasargod, Kerala, India, using GIS techniques. *J. Hazard. Mater. Adv.* 19, 100846.  
613 <https://doi.org/10.1016/j.hazadv.2025.100846>

614 Banach-Szott, M., Debska, B., Rosa, E., 2014. Effect of soil pollution with polycyclic aromatic  
615 hydrocarbons on the properties of humic acids. *Journal of Soils and Sediments* 14, 1169–  
616 1178. <https://doi.org/10.1007/s11368-014-0873-9>.

617 Baragaño, D., Alonso, J., Gallego, J.R., Lobo, M.C., Gil-Díaz, M., 2020. Magnetite  
618 nanoparticles for the remediation of soils co-contaminated with As and PAHs. *Chemical  
619 Engineering Journal* 399, 125809. <https://doi.org/10.1016/j.cej.2020.125809>.

620 Bhattacharyya, R., Kundu, S., Srivastva, A.K., Gupta, H.S., Prakash, V., Bhatt, J.C., 2011. Long  
621 term fertilization effects on soil organic carbon pools in a sandy loam soil of the Indian

622 sub-Himalayas. *Plant and Soil* 341, 109–124. <https://doi.org/10.1007/s11104-010-0627-4>.

623 Bornø, M.L., Müller-Stöver, D.S., Liu, F.L., 2019. Biochar properties and soil type drive the  
624 uptake of macro- and micronutrients in maize (*Zea mays* L.). *Journal of Plant Nutrition*  
625 *and Soil Science* 182, 149–158. <https://doi.org/10.1002/jpln.201800228>.

626 Brown, K.H., Bach, E.M., Drijber, R.A., Hofmockel, K.S., Jeske, E.S., Sawyer, J.E., Castellano,  
627 M.J., 2014. A long-term nitrogen fertilizer gradient has little effect on soil organic matter  
628 in a high-intensity maize production system. *Global Change Biology* 20, 1339–1350.  
629 <https://doi.org/10.1111/gcb.12519>.

630 Burgeon, V., Fouché, J., Garré, S., Dehkordi, R.H., Colinet, G., Cornelis, J.T., 2022. Young and  
631 century-old biochars strongly affect nutrient cycling in a temperate agroecosystem.  
632 *Agriculture, Ecosystems & Environment* 328, 107847.  
633 <https://doi.org/10.1016/j.agee.2021.107847>.

634 Cambardella, C.A., Elliott, E.T., 1992. Particulate soil organic-matter changes across a  
635 grassland cultivation sequence. *Soil Science Society of America Journal* 56, 777–783.  
636 <https://doi.org/10.2136/sssaj1992.03615995005600030017x>.

637 Cao, L.Y., Zhang, X.Y., Xu, Y., Xiang, W., Wang, R., Ding, F.J., Hong, P.Z., Gao, B., 2022.  
638 Straw and wood based biochar for CO<sub>2</sub> capture: Adsorption performance and governing  
639 mechanisms. *Separation and Purification Technology* 287, 120592.  
640 <https://doi.org/10.1016/j.seppur.2022.120592>.

641 Castellano, M.J., Mueller, K.E., Olk, D.C., Sawyer, J.E., Six, J., 2015. Integrating plant litter  
642 quality, soil organic matter stabilization, and the carbon saturation concept. *Global Change*  
643 *Biology* 21, 3200–3209. <https://doi.org/10.1111/gcb.12982>.

644 Chen, H.L., Zhou, J.M., Xiao, B.H., 2010. Characterization of dissolved organic matter derived  
645 from rice straw at different stages of decay. *Journal of Soils and Sediments* 10, 915–922.  
646 <https://doi.org/10.1007/s11368-010-0210-x>.

647 Chen, L.M., Sun, S.L., Zhou, Y.Y., Zhang, B.X., Peng, Y.T., Zhuo, Y.C., Ai, W.K., Gao, C.F.,  
648 Wu, B., Liu, D.W., Sun, C.R., 2023. Straw and straw biochar differently affect fractions  
649 of soil organic carbon and microorganisms in farmland soil under different water regimes.  
650 *Environmental Technology & Innovation* 32, 103412.  
651 <https://doi.org/10.1016/j.eti.2023.103412>.

652 Christensen, B.T., 1992. Physical fractionation of soil and organic matter in primary particle  
653 size and density separates. In: Stewart, B.A. (Ed.), *Advances in Soil Science*. Springer  
654 New York, New York, NY, pp. 1–90. [https://doi.org/10.1007/978-1-4612-2930-8\\_1](https://doi.org/10.1007/978-1-4612-2930-8_1).

655 Connell, R.K., James, T.Y., Blesh, J., 2025. A legume-grass cover crop builds mineral-  
656 associated organic matter across variable agricultural soils. *Soil Biology and Biochemistry*  
657 203, 109726. <https://doi.org/10.1016/j.soilbio.2025.109726>.

658 Cotrufo, M.F., Haddix, M.L., Kroeger, M.E., Stewart, C.E., 2022. The role of plant input  
659 physical-chemical properties, and microbial and soil chemical diversity on the formation  
660 of particulate and mineral-associated organic matter. *Soil Biology and Biochemistry* 168,  
661 108648. <https://doi.org/10.1016/j.soilbio.2022.108648>.

662 Cotrufo, M.F., Soong, J.L., Horton, A.J., Campbell, E.E., Haddix, M.L., Wall, D.H., Parton,  
663 W.J., 2015. Formation of soil organic matter via biochemical and physical pathways of  
664 litter mass loss. *Nature Geoscience* 8, 776–779. <https://doi.org/10.1038/ngeo2520>.

665 Cotrufo, M.F., Wallenstein, M.D., Boot, C.M., Denef, K., Paul, E., 2013. The Microbial

666 Efficiency- Matrix Stabilization (MEMS) framework integrates plant litter decomposition  
667 with soil organic matter stabilization: Do labile plant inputs form stable soil organic matter?  
668 *Global Change Biology* 19, 988–995. <https://doi.org/10.1111/gcb.12113>.

669 Dou, S., Li, K., 2010. Effect of organic matter application on CP-MAS-13C-NMR spectra of  
670 humic acids from a brown soil. In: Xu, J.M., Huang, P.M. (Eds.), *Molecular  
671 Environmental Soil Science at the Interfaces in the Earth's Critical Zone*. Springer Berlin  
672 Heidelberg, Berlin, Heidelberg, pp. 29–31. [https://doi.org/10.1007/978-3-642-05297-2\\_9](https://doi.org/10.1007/978-3-642-05297-2_9).

673 Dou, S., Shan, J., Song, X.Y., Cao, R., Wu, M., Li, C.L., Guan, S., 2020. Are humic substances  
674 soil microbial residues or unique synthesized compounds? A perspective on their  
675 distinctiveness. *Pedosphere* 30, 159–167. [https://doi.org/10.1016/S1002-0160\(20\)60001-](https://doi.org/10.1016/S1002-0160(20)60001-7)  
676 [7](https://doi.org/10.1016/S1002-0160(20)60001-7).

677 Duan, L.C., Wang, Q.H., Li, J.N., Wang, F.H., Yang, H., Guo, B.L., Hashimoto, Y., 2022. Zero  
678 valent iron or Fe<sub>3</sub>O<sub>4</sub>-loaded biochar for remediation of Pb contaminated sandy soil:  
679 Sequential extraction, magnetic separation, XAFS and ryegrass growth. *Environmental  
680 Pollution* 308, 119702. <https://doi.org/10.1016/j.envpol.2022.119702>.

681 Dungait, J.A.J., Hopkins, D.W., Gregory, A.S., Whitmore, A.P., 2012. Soil organic matter  
682 turnover is governed by accessibility not recalcitrance. *Global Change Biology* 18, 1781–  
683 1796. <https://doi.org/10.1111/j.1365-2486.2012.02665.x>.

684 Fan, Y.V., Klemes, J.J., Lee, C.T., 2021. Environmental performance and techno-economic  
685 feasibility of different biochar applications: An overview. *Chemical Engineering  
686 Transactions* 83, 469–474. <https://doi.org/10.3303/CET2183079>.

687 Feng, H.L., Han, X.Z., Biswas, A., Zhang, M., Zhu, Y.C., Ji, Y.X., Lu, X.C., Chen, X., Yan, J.,

688 Zou, W.X., 2025. Long-term organic material application enhances black soil productivity  
689 by improving aggregate stability and dissolved organic matter dynamics. *Field Crops*  
690 *Research* 328, 109946. <https://doi.org/10.1016/j.fcr.2025.109946>.

691 Guo, X.W., Viscarra Rossel, R.A., Wang, G.C., Xiao, L.J., Wang, M.M., Zhang, S., Luo, Z.K.,  
692 2022. Particulate and mineral-associated organic carbon turnover revealed by modelling  
693 their long-term dynamics. *Soil Biology and Biochemistry* 173, 108780.  
694 <https://doi.org/10.1016/j.soilbio.2022.108780>.

695 He, W., Wang, H., Ye, W.H., Tian, Y.L., Hu, G.Q., Lou, Y.H., Pan, H., Yang, Q.G., Zhuge, Y.P.,  
696 2022. Distinct stabilization characteristics of organic carbon in coastal salt-affected soils  
697 with different salinity under straw return management. *Land Degradation & Development*  
698 33, 2246–2257. <https://doi.org/10.1002/ldr.4276>.

699 Hua, F.Y., Bruijnzeel, L.A., Meli, P., Martin, P.A., Zhang, J., Nakagawa, S., Miao, X., Wang,  
700 W., McEvoy, C., Peña-Arancibia, J.L., Brancalion, P.H.S., Smith, P., Edwards, D.P.,  
701 Balmford, A., 2022. The biodiversity and ecosystem service contributions and trade-offs  
702 of forest restoration approaches. *Science* 376, 839–844.  
703 <https://doi.org/10.1126/science.abl4649>.

704 Janzen, H.H., 2015. Beyond carbon sequestration: soil as conduit of solar energy. *European J*  
705 *Soil Science* 66, 19–32. <https://doi.org/10.1111/ejss.12194>.

706 Khaledi, S., Delbari, M., Galavi, H., Bagheri, H., Chari, M.M., 2023. Effects of biochar particle  
707 size, biochar application rate, and moisture content on thermal properties of an unsaturated  
708 sandy loam soil. *Soil and Tillage Research* 226, 105579.  
709 <https://doi.org/10.1016/j.still.2022.105579>.

710 Kleber, M., Sollins, P., Sutton, R., 2007. A conceptual model of organo-mineral interactions in  
711 soils: Self-assembly of organic molecular fragments into zonal structures on mineral  
712 surfaces. *Biogeochemistry* 85, 9–24. <https://doi.org/10.1007/s10533-007-9103-5>.

713 Lavallee, J.M., Soong, J.L., Cotrufo, M.F., 2020. Conceptualizing soil organic matter into  
714 particulate and mineral-associated forms to address global change in the 21st century.  
715 *Global Change Biology* 26, 261–273. <https://doi.org/10.1111/gcb.14859>.

716 Li, X.N., Li, R.P., Zhan, M.Q., Hou, Q., Zhang, H.Y., Wu, G.Q., Ding, L.Q., Lv, X.F., Xu, Y.,  
717 2024. Combined magnetic biochar and ryegrass enhanced the remediation effect of soils  
718 contaminated with multiple heavy metals. *Environment International* 185, 108498.  
719 <https://doi.org/10.1016/j.envint.2024.108498>.

720 Liang, J.J., Crowther, T.W., Picard, N., Wisser, S., Zhou, M., Alberti, G., Schulze, E.D., McGuire,  
721 A.D., Bozzato, F., Pretzsch, H., de-Miguel, S., Paquette, A., Hérault, B., Scherer-Lorenzen,  
722 M., Barrett, C.B., Glick, H.B., Hengeveld, G.M., Nabuurs, G.J., Pfautsch, S., Viana, H.,  
723 Vibrans, A.C., Ammer, C., Schall, P., Verbyla, D., Tchebakova, N., Fischer, M., Watson,  
724 J.V., Chen, H.Y.H., Lei, X., Schelhaas, M.J., Lu, H., Gianelle, D., Parfenova, E.I., Salas,  
725 C., Lee, E., Lee, B., Kim, H.S., Bruelheide, H., Coomes, D.A., Piotta, D., Sunderland, T.,  
726 Schmid, B., Gourlet-Fleury, S., Sonké, B., Tavani, R., Zhu, J., Brandl, S., Vayreda, J.,  
727 Kitahara, F., Searle, E.B., Neldner, V.J., Ngugi, M.R., Baraloto, C., Frizzera, L., Bałazy,  
728 R., Oleksyn, J., Zawila-Niedzwiecki, T., Bouriaud, O., Bussotti, F., Finér, L., Jaroszewicz,  
729 B., Jucker, T., Valladares, F., Jagodzinski, A.M., Peri, P.L., Gonmadje, C., Marthy, W.,  
730 O'Brien, T., Martin, E.H., Marshall, A.R., Rovero, F., Bitariho, R., Niklaus, P.A., Alvarez-  
731 Loayza, P., Chamuya, N., Valencia, R., Mortier, F., Wortel, V., Engone-Obiang, N.L.,

732 Ferreira, L.V., Odeke, D.E., Vasquez, R.M., Lewis, S.L., Reich, P.B., 2016. Positive  
733 biodiversity-productivity relationship predominant in global forests. *Science* 354, aaf8957.  
734 <https://doi.org/10.1126/science.aaf8957>.

735 Liu, J.X., Sun, P., Chen, Y.Y., Guo, J.M., Liu, L.C., Zhao, X.Y., Xin, J., Liu, X.L., 2024. The  
736 regulation pathways of biochar and microorganism in soil-plant system by multiple  
737 statistical methods: The forms of carbon participation in coastal wetlands. *Chemosphere*  
738 362, 142918. <https://doi.org/10.1016/j.chemosphere.2024.142918>.

739 Mitchell, E., Scheer, C., Rowlings, D., Conant, R.T., Cotrufo, M.F., Grace, P., 2018. Amount  
740 and incorporation of plant residue inputs modify residue stabilisation dynamics in soil  
741 organic matter fractions. *Agriculture, Ecosystems & Environment* 256, 82–91.  
742 <https://doi.org/10.1016/j.agee.2017.12.006>.

743 Mohammed, I., Kodaolu, B., Zhang, T.Q., Wang, Y.T., Audette, Y., Longstaffe, J., 2023.  
744 Analysis of molecular structure changes in humic acids from manure-amended soils over  
745 17 years using elemental analysis and solid-state <sup>13</sup>C nuclear magnetic resonance  
746 spectroscopy. *Soil Systems* 7, 76. <https://doi.org/10.3390/soilsystems7030076>.

747 Ndzelu, B.S., Dou, S., Zhang, X.W., Zhang, Y.F., Ma, R., Liu, X., 2021. Tillage effects on  
748 humus composition and humic acid structural characteristics in soil aggregate-size  
749 fractions. *Soil and Tillage Research* 213, 105090.  
750 <https://doi.org/10.1016/j.still.2021.105090>.

751 Nelson, D.W., Sommers, L.E., 1982. Total carbon, organic carbon, and organic matter. In: Page,  
752 A.L. (Ed.), *Methods of Soil Analysis: Part 2 Chemical and Microbiological Properties*.  
753 Wiley, Hoboken, pp. 539–579. <https://doi.org/10.2134/agronmonogr9.2.2ed.c29>.

754 Panda, S., Devi, N., Maiti, P., Chatterjee, A., Hazra P., Singh, V., Parmar, P., Meikap, B., 2026.  
755 Development of a novel FeCl<sub>3</sub>-activated magnetic biochar for adsorptive removal of  
756 paracetamol and environmental impact analysis. *Powder Technology* 470, 122021.  
757 <https://doi.org/10.1016/j.powtec.2025.122021>.

758 Papageorgiou, A., Azzi, E.S., Enell, A., Sundberg, C., 2021. Biochar produced from wood  
759 waste for soil remediation in Sweden: Carbon sequestration and other environmental  
760 impacts. *Science of The Total Environment* 776, 145953.  
761 <https://doi.org/10.1016/j.scitotenv.2021.145953>.

762 Pathy, A., Pokharel, P., Chen, X.L., Balasubramanian, P., Chang, S.X., 2023. Activation  
763 methods increase biochar's potential for heavy-metal adsorption and environmental  
764 remediation: A global meta-analysis. *Science of The Total Environment* 865, 161252.  
765 <https://doi.org/10.1016/j.scitotenv.2022.161252>.

766 Powelson, D.S., Stirling, C.M., Jat, M.L., Gerard, B.G., Palm, C.A., Sanchez, P.A., Cassman,  
767 K.G., 2014. Limited potential of no-till agriculture for climate change mitigation. *Nature*  
768 *Climate Change* 4, 678–683. <https://doi.org/10.1038/nclimate2292>.

769 Rana, P., Soni, V., Sharma, S., Poonia, K., Patial, S., Singh, P., Selvasembian, R., Chaudhary,  
770 V., Hussain, C.M., Raizada, P., 2025. Harnessing nitrogen doped magnetic biochar for  
771 efficient antibiotic adsorption and degradation. *Journal of Industrial and Engineering*  
772 *Chemistry* 148, 174–195. <https://doi.org/10.1016/j.jiec.2025.01.025>.

773 Ren, Z.G., Zhang, H.Y., Wang, Y.W., Lu, L., Ren, D., Wang, J.J., 2021. Multiple roles of  
774 dissolved organic matter released from decomposing rice straw at different times in  
775 organic pollutant photodegradation. *Journal of Hazardous Materials* 401, 123434.

776 <https://doi.org/10.1016/j.jhazmat.2020.123434>.

777 Rocci, K.S., Lavalley, J.M., Stewart, C.E., Cotrufo, M.F., 2021. Soil organic carbon response  
778 to global environmental change depends on its distribution between mineral-associated  
779 and particulate organic matter: A meta-analysis. *Science of The Total Environment* 793,  
780 148569. <https://doi.org/10.1016/j.scitotenv.2021.148569>.

781 Shi, H.Q., Liu, G., An, X.B., Zhao, Y.J., Zheng, F.L., Li, H.R., Zhang, X.C. (John), Pan, X.C.,  
782 Wu, B.L., Wang, X.S., 2024. Tracing soil erosion with Fe<sub>3</sub>O<sub>4</sub> magnetic powder: Principle  
783 and application. *International Soil and Water Conservation Research* 12, 419–431.  
784 <https://doi.org/10.1016/j.iswcr.2023.08.002>.

785 Shi, R.Y., Ni, N., Wang, R.H., Nkoh, J.N., Pan, X.Y., Dong, G., Xu, R.K., Cui, X.M., Li, J.Y.,  
786 2023. Dissolved biochar fractions and solid biochar particles inhibit soil acidification  
787 induced by nitrification through different mechanisms. *Science of The Total Environment*  
788 874, 162464. <https://doi.org/10.1016/j.scitotenv.2023.162464>.

789 Slessarev, E.W., Chadwick, O.A., Sokol, N.W., Nuccio, E.E., Pett-Ridge, J., 2022. Rock  
790 weathering controls the potential for soil carbon storage at a continental scale.  
791 *Biogeochemistry* 157, 1–13. <https://doi.org/10.1007/s10533-021-00859-8>.

792 Sokol, N.W., Whalen, E.D., Jilling, A., Kallenbach, C., Pett-Ridge, J., Georgiou, K., 2022.  
793 Global distribution, formation and fate of mineral-associated soil organic matter under a  
794 changing climate: A trait-based perspective. *Functional Ecology* 36, 1411–1429.  
795 <https://doi.org/10.1111/1365-2435.14040>.

796 Stewart, C.E., Follett, R.F., Wallace, J., Pruessner, E.G., 2012. Impact of biosolids and tillage  
797 on soil organic matter fractions: Implications of carbon saturation for conservation

798 management in the virginia coastal plain. *Soil Science Society of America Journal* 76,  
799 1257–1267. <https://doi.org/10.2136/sssaj2011.0165>.

800 Vendig, I., Guzman, A., De La Cerda, G., Esquivel, K., Mayer, A.C., Ponisio, L., Bowles, T.M.,  
801 2023. Quantifying direct yield benefits of soil carbon increases from cover cropping.  
802 *Nature Sustainability* 6, 1125–1134. <https://doi.org/10.1038/s41893-023-01131-7>.

803 Von Lützow, M., Kögel-Knabner, I., Ekschmitt, K., Flessa, H., Guggenberger, G., Matzner, E.,  
804 Marschner, B., 2007. SOM fractionation methods: Relevance to functional pools and to  
805 stabilization mechanisms. *Soil Biology and Biochemistry* 39, 2183–2207.  
806 <https://doi.org/10.1016/j.soilbio.2007.03.007>.

807 Wang, J.S., Li, S.C., Yin, H.M., Riaz, M., Liu, X.W., Zhang, M.Y., 2025. Biochar suppresses  
808 Clubroot disease in Chinese cabbage by improving soil nutrient conditions and recruiting  
809 beneficial microorganisms. *Applied Soil Ecology* 210, 106107.  
810 <https://doi.org/10.1016/j.apsoil.2025.106107>.

811 Witzgall, K., Vidal, A., Schubert, D.I., Höschel, C., Schweizer, S.A., Buegger, F., Pouteau, V.,  
812 Chenu, C., Mueller, C.W., 2021. Particulate organic matter as a functional soil component  
813 for persistent soil organic carbon. *Nature Communications* 12, 4115.  
814 <https://doi.org/10.1038/s41467-021-24192-8>.

815 Wood, S.A., Sokol, N., Bell, C.W., Bradford, M.A., Naeem, S., Wallenstein, M.D., Palm, C.A.,  
816 2016. Opposing effects of different soil organic matter fractions on crop yields. *Ecological*  
817 *Applications* 26, 2072–2085. <https://doi.org/10.1890/16-0024.1>.

818 Xie, H.T., Li, J.W., Zhu, P., Peng, C., Wang, J.K., He, H.B., Zhang, X.D., 2014. Long-term  
819 manure amendments enhance neutral sugar accumulation in bulk soil and particulate

820 organic matter in a Mollisol. *Soil Biology and Biochemistry* 78, 45–53.  
821 <https://doi.org/10.1016/j.soilbio.2014.07.009>.

822 Xu, C.B., Tan, X., Zhao, J.W., Cao, J.M., Ren, M., Xiao, Y., Lin, A.J., 2021. Optimization of  
823 biochar production based on environmental risk and remediation performance: Take  
824 kitchen waste for example. *Journal of Hazardous Materials* 416, 125785.  
825 <https://doi.org/10.1016/j.jhazmat.2021.125785>.

826 Xu, S., Chen, Z., Zhang, N., Li, Y., Xu, Y., Ding, W., 2026. Soil carbon quality determined the  
827 responses of respiration components to nitrogen fertilization and straw return. *Soil Tillage  
828 Res.* 259, 107072. <https://doi.org/10.1016/j.still.2026.107072>

829 Yin, J.X., Zhao, L., Xu, X.Y., Li, D.P., Qiu, H., Cao, X.D., 2022. Evaluation of long-term  
830 carbon sequestration of biochar in soil with biogeochemical field model. *Science of The  
831 Total Environment* 822, 153576. <https://doi.org/10.1016/j.scitotenv.2022.153576>.

832 Yu, W.J., Huang, W.J., Weintraub-Leff, S.R., Hall, S.J., 2022. Where and why do particulate  
833 organic matter (POM) and mineral-associated organic matter (MAOM) differ among  
834 diverse soils? *Soil Biology and Biochemistry* 172, 108756.  
835 <https://doi.org/10.1016/j.soilbio.2022.108756>.

836 Zhang, B.L., Jin, Y.P., Qi, J.X., Chen, H., Chen, G., Tang, S.S., 2021. Porous carbon materials  
837 based on *Physalis alkekengi* L. husk and its application for removal of malachite green.  
838 *Environmental Technology & Innovation* 21, 101343.  
839 <https://doi.org/10.1016/j.eti.2020.101343>.

840 Zhang, B.L., Li, R.Q., Zheng, Y.Y., Chen, S.J., Su, Y.J., Zhou, W., Sui, Q., Liang, D.D., 2024.  
841 Biochar composite with enhanced performance prepared through microbial modification

842 for water pollutant removal. *International Journal of Molecular Sciences* 25, 11732.  
843 <https://doi.org/10.3390/ijms252111732>.

844 Zhang, G.X., Ren, R., Yan, X.R., Zhu, Y., Zhang, H.Y., Yan, G.Y., 2025. The key role of  
845 magnetic iron-to-biochar mass ratios in the dissipation of oxytetracycline and its  
846 resistance genes in soils with and without biodegradable microplastics. *Journal of*  
847 *Environmental Management* 377, 124658.  
848 <https://doi.org/10.1016/j.jenvman.2025.124658>.

849 Zhou, J.Y., Liu, Y.Y., Han, Y.T., Jing, F.Q., Chen, J.W., 2019. Bone-derived biochar and  
850 magnetic biochar for effective removal of fluoride in groundwater: Effects of synthesis  
851 method and coexisting chromium. *Water Environment Research* 91, 588–597.  
852 <https://doi.org/10.1002/wer.1068>.